

A radio continuum study of the Magellanic Clouds

VIII. Discrete sources common to radio and infrared surveys of the Magellanic Clouds

M.D. Filipović^{1,2,3}, P.A. Jones¹, G.L. White¹, and R.F. Haynes^{3,1}

¹ University of Western Sydney, Nepean, P.O. Box 10, Kingswood, NSW 2747, Australia

e-mail: M.Filipovic@uws.edu.au; p.jones@nepean.uws.edu.au; g.white@nepean.uws.edu.au

² Max-Planck-Institut für extraterrestrische Physik, Giessenbachstraße, D-85740 Garching, Germany

³ Australia Telescope National Facility, CSIRO, P.O. Box 76, Epping, NSW 2121, Australia

e-mail: mfilipovic@atnf.csiro.au; rhaynes@atnf.csiro.au

Received November 28; accepted December 24, 1997

Abstract. We compare Parkes Telescope radio surveys with the IRAS Infrared (IR) surveys of the Magellanic Clouds (MCs). We find 130 discrete sources in common towards the Large Magellanic Cloud (LMC) with both radio and IR emission. These 130 sources are mainly H II regions (89) and supernova remnants (21). For 12 of the sources we have no identification and eight are background objects. We find 38 sources in common for the Small Magellanic Cloud (SMC). Most of these sources are intrinsic (31) to the SMC, five sources are previously known background galaxies and two sources remain ambiguous.

A flux density comparison of the radio and IR sources shows very good correlation and we note that the strongest sources at both radio and IR frequencies are H II regions. From the radio–IR comparison we propose that some 40 new sources in the LMC and 10 in the SMC are H II regions or SNRs. All these new sources are also identified in optical surveys.

Key words: galaxies: Magellanic Clouds — radio continuum: galaxies — infrared: galaxies — ISM: H II regions — ISM: supernova remnants (SNRs) — galaxies: ISM

1. Introduction

In this paper we compare sources common to the Parkes radio surveys and the Infra-Red Astronomical Satellite (IRAS) surveys using primarily the radio results of Filipović et al. (1995; hereafter Paper IV), Filipović et al. (1996; hereafter Paper IVa), Filipović et al. (1997; hereafter Paper V) and the IR catalogues of Schwering &

Israel (1990; see also Schwering & Israel 1989; Schwering 1989). We classify each source as either an H II region, supernova remnant (SNR) or background object.

In Sect. 2 we discuss briefly radio and infrared (IR) observations of discrete sources towards the MCs. In Sects. 3 and 4 we analyse and discuss all discrete sources common to the radio and IR surveys. In Sect. 5 we classify previously unknown sources from the field of the MCs and, finally, in Sect. 6 we discuss the radio–to–IR flux relationships for all sources in common towards the MCs.

2. Discrete sources towards the Magellanic Clouds

2.1. Radio data

Catalogues of discrete radio sources towards the LMC at six radio frequencies are presented in Papers IV and IVa of this series and in Filipović (1996). The total number of catalogued radio sources is 483. The common area of the radio and IR surveys (~ 100 square degrees) lies between RA (B1950)= $04^{\text{h}}23^{\text{m}}$ to $06^{\text{h}}14^{\text{m}}$ and Dec (B1950)= -64° to -74° .

The new catalogues of radio sources in the SMC at five radio frequencies are given in Paper V and in Filipović (1996). There is a total of 224 radio sources towards the SMC. The area that these catalogues cover is ~ 42 square degrees between RA (B1950)= $00^{\text{h}}12^{\text{m}}$ to $01^{\text{h}}38^{\text{m}}$ and Dec (B1950)= $-69^{\circ}40'$ to $-76^{\circ}20'$.

As clear radio detections, we listed only radio sources that are stronger than 5σ or seen in at least two frequencies.

2.2. Infrared data

The IRAS surveyed in a uniform fashion most of the sky in four photometric bands centred at 12, 25, 60 and $100\ \mu\text{m}$.

These observations provide a remarkable data-base for investigating discrete sources, star-formation regions and dust properties in galaxies. This is because the mid- and far-infrared (MIR and FIR) emission from galaxies, as measured by IRAS, is mostly caused by thermal radiation from interstellar dust grains heated by starlight. The MIR and FIR thus probe directly the dust properties, the mix of dust temperatures and young stellar populations responsible for most of the dynamics in the interstellar radiation field.

An atlas and catalogues of IR sources in the MCs were published by Schwering & Israel (1990) and further information about MC IR surveys can be found there. Altogether, some 1891 LMC and 249 SMC sources were listed in this study. Also as a check on the Schwering & Israel (1990) catalogues we have used the IRAS FITS images obtained from Skyview (<http://skview.gsfc.nasa.gov/skyview.html>).

The angular resolution of the IRAS maps of the MCs was not precisely known, owing to their special beam pattern (Meylnik & Rice 1990). Because of the method used to deconvolve the dirty IRAS beam it was known only that the maps at four IR frequencies have equal resolution. On this assumption and the known positions of K and M stars from the SAO catalogue we fitted some of the bright stars in the 12- μm image with a two-dimensional Gaussian fitting routine. The resolution derived by this method is 3.7' for the original maps.

A large fraction of sources listed in Schwering & Israel (1990) catalogues could not be identified in the IRAS FITS images. Therefore, it is very difficult to estimate a number of sources that have positional coincidence by chance alignment.

3. Radio-to-infrared comparison of the sources towards the LMC

3.1. Source identification

The comparison of the radio and IR surveys resulted in the discovery of 130 sources common to both surveys. The basic criterion for positive source identification is that a source must lie within 2.5' of its counterpart. The most accurate radio positions available are from the highest radio-frequency survey on which the source appears. These positions were compared with IR positions from Schwering & Israel (1990).

Data for these 130 sources in common are presented in Table 1. Columns 2 and 3 give the radio source and IRAS source names respectively. Column 4 lists the source radio flux density at 4.75 GHz. For 12 sources the flux density at 4.75 GHz was estimated by interpolation from other radio frequencies; these sources are flagged in Col. 4.

The IR data, that is the flux at 60 μm and the IR spectral index (α_{IR}), are listed for each source in Col. 5

and Col. 7 respectively. Estimates of the α_{IR} of each IR source are based on flux densities listed in Schwering & Israel (1990). The IR spectral index is defined by the relationship $S_\nu \sim \nu^\alpha$, where S_ν is the flux density and ν is the frequency. The integrated flux densities at the various IR frequencies were plotted as $\text{Log}(S_\nu)$ versus $\text{Log}(\nu_{\mu\text{m}})$ and (for most sources) straight lines were fitted with a simple linear regression to produce the best estimates of spectral index.

Column 6 lists the source radio spectral index (α_{RAD}) and error ($\Delta\alpha_{\text{RAD}}$) defined as for the IR spectral index in the previous paragraph. Radio spectral indices are not given for 13 sources which were detected at only one radio frequency. For one IR source no IR spectral index is given since it was detected at only one IR frequency.

Column 8 of Table 1 gives the "radio source type". Sources are denoted as BG (background sources), HII regions and SNRs. Note that upper case letters (BG, SNR and HII) are used for classifications from previous works and lower case (bg, hii and snr) for sources classified here. The question-mark indicates probable but not certain classification. The criteria by which we classify these sources are discussed in Sect. 5 and in Filipović et al. (1998a; hereafter Paper VII). Other source names can be found in Papers IV, V and VI.

3.2. Positional differences between the LMC radio and infrared sources

Positional comparisons were undertaken for all 130 sources common to the radio and IR surveys. The results of this comparison are shown in Figs. 1a and 1b. For the 130 sources, the mean difference in RA is $16'' \pm 5''$ (radio-IR) with standard deviation (SD) of $54''$. The difference in Dec is $4'' \pm 5''$ (SD= $53''$). This uncertainty is consistent with the combined positional uncertainties for the radio (defined in Paper IV) and the IR sources, and retrospectively justifies the initial identification criterion of 2.5' (which is equivalent to 2.8σ in both RA and Dec). Figure 1b shows that there is an excess in the number of sources with small radio-IR differences, as expected, well above the number due to random coincidence.

4. Radio-to-infrared comparison of the sources towards the SMC

4.1. Source identification

In the same manner as for the LMC, radio and IR surveys of the SMC have been compared, resulting in the identification of 38 sources common to both surveys. Each radio source and IR counterpart lie within 2.5' of each other. This criterion was chosen according to the upper limit of positional uncertainties in our 1.42-GHz survey (Paper V).

Table 1. Catalogue of the LMC radio sources identified in the IRAS survey. The IR source number (Col. 3) is taken from Schwering & Israel (1990)

(1) No.	(2) Radio Source Name	(3) IR Source Name	(4) $S_{4.75}$ (Jy)	(5) $S_{60\mu\text{m}}$ (Jy)	(6) $\alpha_{\text{RAD}} \pm \Delta\alpha_{\text{RAD}}$	(7) $\alpha_{\text{IR}} \pm \Delta\alpha_{\text{IR}}$	(8) Type
1.	LMC B0433–7139	LI-LMC 1836	0.098*	0.4	-1.05 ± 0.16		bg
2.	LMC B0443–6801	LI-LMC 1858	0.047	0.8	-0.53 ± 0.06	-2.14 ± 0.06	BG
3.	LMC B0449–6917	LI-LMC 58 (63)	0.249	62.1	-0.46 ± 0.20	-2.11 ± 0.06	H II
4.	LMC B0450–6745	LI-LMC 65	0.105	4.6	-0.07 ± 0.21	-2.64 ± 0.19	H II
5.	LMC B0450–6927	LI-LMC 70	0.267	4.1	-0.68 ± 0.16	-2.10 ± 0.28	SNR?
6.	LMC B0452–6700	LI-LMC 102	0.339	116.7	-0.20 ± 0.06	-1.96 ± 0.12	H II
7.	LMC B0452–6722	LI-LMC 112	0.096	10.3	-0.10 ± 0.08	-2.50 ± 0.17	hii
8.	LMC B0452–6924	LI-LMC 115 (107)	0.012*	18.6		-1.62 ± 0.02	hii
9.	LMC B0452–6927	LI-LMC 103 (107)	1.843	343.6	-0.06 ± 0.01	-1.78 ± 0.24	H II
10.	LMC B0453–6700	LI-LMC 132	0.049	5.4	-0.55 ± 0.08	-2.00 ± 0.26	SNR
11.	LMC B0453–6807	LI-LMC 122 (129)	0.157	35.6	-0.48 ± 0.06	-2.02 ± 0.11	hii
12.	LMC B0453–6917	LI-LMC 121	0.077	24.8	-0.14 ± 0.02	-1.45 ± 0.08	H II
13.	LMC B0454–6716	LI-LMC 166	0.302	8.3	-0.23 ± 0.08	-2.17 ± 0.30	H II
14.	LMC B0454–6916	LI-LMC 148 (162)	0.621	178.0	0.09 ± 0.06	-2.09 ± 0.14	H II
15.	LMC B0456–6629	LI-LMC 217 (210)	3.722	244.3	0.05 ± 0.06	-2.29 ± 0.12	H II
16.	LMC B0456–6636	LI-LMC 214 (219)	0.683	37.3	0.14 ± 0.04	-2.22 ± 0.07	H II
17.	LMC B0456–7019	LI-LMC 221	0.103	2.5	-0.32 ± 0.05	-2.21 ± 0.51	BG
18.	LMC B0457–6632	LI-LMC 243 (248)	0.641	62.1	-0.09 ± 0.04	-2.28 ± 0.34	H II
19.	LMC B0457–6830	LI-LMC 235	0.452	118.0	-0.09 ± 0.06	-2.15 ± 0.10	H II
20.	LMC B0457–6849	LI-LMC 232	0.124	47.6	-0.50 ± 0.14	-2.13 ± 0.10	hii
21.	LMC B0458–6616	LI-LMC 257	0.114	13.2	-1.08 ± 0.08	-2.55 ± 0.26	hii
22.	LMC B0458–6626	LI-LMC 251	0.306	33.1	-0.38 ± 0.11	-2.12 ± 0.10	H II
23.	LMC B0459–6612	LI-LMC 289		2.5		-2.16 ± 0.36	SNR?
24.	LMC B0459–6620	LI-LMC 290	0.080	8.3		-1.94 ± 0.05	hii
25.	LMC B0500–6802	LI-LMC 292	0.056	2.1	-0.75 ± 0.12	-1.83 ± 0.16	hii
26.	LMC B0500–7014	LI-LMC 295	0.190	21.5	-0.71 ± 0.19	-2.48 ± 0.28	SNR
27.	LMC B0502–6908	LI-LMC 347	0.075	2.9	-0.64 ± 0.10	-1.39 ± 0.41	?
28.	LMC B0502–6935	LI-LMC 340	0.139	2.1	-1.24 ± 0.06	-2.13 ± 0.26	BG
29.	LMC B0503–6715	LI-LMC 364 (356)	0.042*	2.1		-1.79 ± 0.46	?
30.	LMC B0503–6722	LI-LMC 371 (375)	0.090	31.9	-1.99 ± 0.22	-2.14 ± 0.07	hii
31.	LMC B0505–6659	LI-LMC 414	0.107	31.9	-0.19 ± 0.05	-2.01 ± 0.29	H II
32.	LMC B0505–6740	LI-LMC 404 (416)	0.236	5.8	-0.12 ± 0.10	-2.12 ± 0.14	hii
33.	LMC B0505–6807	LI-LMC 405 (411)	0.306	25.3	-0.29 ± 0.16	-2.39 ± 0.11	H II
34.	LMC B0505–7010	LI-LMC 412 (417)	0.210	24.8	-0.62 ± 0.12	-2.19 ± 0.09	hii
35.	LMC B0505–7048	LI-LMC 399	0.145	22.8	-0.03 ± 0.04	-2.17 ± 0.11	hii
36.	LMC B0505–7058	LI-LMC 409	0.064	62.9	-0.46 ± 0.05	-1.92 ± 0.20	hii
37.	LMC B0506–6812	LI-LMC 447	0.089	7.5	-0.69 ± 0.23	-2.25 ± 0.20	hii
38.	LMC B0509–6848	LI-LMC 510	0.529	14.5	-0.56 ± 0.09	-2.23 ± 0.23	SNR
39.	LMC B0510–6758	LI-LMC 525 (545)	0.062	3.3	-0.15 ± 0.07	-2.26 ± 0.30	H II
40.	LMC B0510–6857	LI-LMC 534	1.156	314.6	0.00 ± 0.05	-1.99 ± 0.19	H II
41.	LMC B0512–6710	LI-LMC 599	0.089	6.2		-2.17 ± 0.26	?
42.	LMC B0512–7028	LI-LMC 620	0.052	19.0	-0.83 ± 0.08	-1.80 ± 0.17	hii
43.	LMC B0513–6729	LI-LMC 642	0.186	60.9	-0.48 ± 0.02	-2.12 ± 0.14	?hii
44.	LMC B0513–6915	LI-LMC 636	0.264	16.6	-0.45 ± 0.16	-1.58 ± 0.18	SNR
45.	LMC B0513–6920	LI-LMC 640	0.162*	12.4	-0.10 ± 0.04	-2.42 ± 0.22	H II
46.	LMC B0513–6925	LI-LMC 635	1.099	256.7	-0.09 ± 0.04	-1.91 ± 0.21	H II
47.	LMC B0514–6711	LI-LMC 641	0.129	4.1	-0.82 ± 0.10	-1.96 ± 0.28	hii
48.	LMC B0514–6932	LI-LMC 665	0.197	18.6	-0.05 ± 0.01	-2.64 ± 0.28	hii
49.	LMC B0516–6722	LI-LMC 723	0.053	9.5	0.10 ± 0.09	-1.99 ± 0.15	hii
50.	LMC B0518–7117	LI-LMC 766	0.169	49.4	0.00 ± 0.05	-1.88 ± 0.13	hii
51.	LMC B0519–6916	LI-LMC 789	0.931	58.0	-0.18 ± 0.06	-2.06 ± 0.19	H II
52.	LMC B0519–6941	LI-LMC 804 (816)	0.866	124.2	-0.42 ± 0.06	-2.19 ± 0.12	SNR
53.	LMC B0520–6649	LI-LMC 831	0.093	18.2	-0.12 ± 0.09	-2.33 ± 0.16	hii
54.	LMC B0520–6655	LI-LMC 823	0.042	27.3		-2.30 ± 0.18	hii
55.	LMC B0521–6545	LI-LMC 878	0.141	11.3	-0.23 ± 0.10	-1.97 ± 0.41	SNR?
56.	LMC B0521–6851	LI-LMC 847	0.151	11.6	-0.96 ± 0.17	-2.16 ± 0.41	?
57.	LMC B0521–7002	LI-LMC 866	0.071	9.1	-0.47 ± 0.04	-1.81 ± 0.24	BG
58.	LMC B0522–6643	LI-LMC 900	0.095	17.8	-0.82 ± 0.06	-2.16 ± 0.12	hii
59.	LMC B0522–6757	LI-LMC 894	0.236	70.4	-0.02 ± 0.08	-2.03 ± 0.30	SNR
60.	LMC B0522–6800	LI-LMC 880 (876, 887)	1.666	246.3	-0.52 ± 0.07	-2.13 ± 0.22	H II
61.	LMC B0522–6942	LI-LMC 872	0.174	66.2	-0.75 ± 0.04	-1.88 ± 0.20	H II
62.	LMC B0523–6806	LI-LMC 911	0.580	89.0	-0.10 ± 0.08	-1.71 ± 0.18	H II
63.	LMC B0523–6953	LI-LMC 921	0.021	18.6		-2.34 ± 0.19	hii
64.	LMC B0523–7138	LI-LMC 910 (929)	0.176	9.1	-0.86 ± 0.05	-2.34 ± 0.09	SNR?
65.	LMC B0524–6627	LI-LMC 983		13.7	-0.33 ± 0.06	-2.46 ± 0.32	SNR

Table 1. continued

(1) No.	(2) Radio Source Name	(3) IR Source Name	(4) $S_{4.75}$ (Jy)	(5) $S_{60\mu\text{m}}$ (Jy)	(6) $\alpha_{\text{RAD}} \pm \Delta\alpha_{\text{RAD}}$	(7) $\alpha_{\text{IR}} \pm \Delta\alpha_{\text{IR}}$	(8) Type
66.	LMC B0524–6834	LI-LMC 979	0.012*	3.3		-1.61 ± 0.38	hii
67.	LMC B0524–7121	LI-LMC 960	0.104	5.0	-0.48 ± 0.14	-2.51 ± 0.34	SNR?
68.	LMC B0525–6607	LI-LMC 1022 (1038)	1.009	19.5	-0.51 ± 0.06	-2.13 ± 0.12	SNR
69.	LMC B0525–6618	LI-LMC 1015 (1009)	1.173	91.1	-0.41 ± 0.07	-2.15 ± 0.06	H II
70.	LMC B0525–6831	LI-LMC 999 (978)	0.287	39.3	-0.52 ± 0.16	-2.09 ± 0.07	H II
71.	LMC B0525–6954	LI-LMC 1021 (993, 1025)	0.032	20.7		-2.21 ± 0.40	?
72.	LMC B0526–6558	LI-LMC 1042 (1067)	0.119	2.1	-0.61 ± 0.06	-2.05 ± 0.28	?
73.	LMC B0526–6712	LI-LMC 1017	0.167	8.7	-0.02 ± 0.21	-2.22 ± 0.19	hii
74.	LMC B0526–6731	LI-LMC 1045 (1037)	1.745	8.3	-0.27 ± 0.08	-2.13 ± 0.08	H II
75.	LMC B0526–6740	LI-LMC 1043 (1052)	0.380	11.6	0.12 ± 0.22	-2.25 ± 0.13	H II
76.	LMC B0526–6751	LI-LMC 1068	0.159	4.6	-0.80 ± 0.28	-2.18 ± 0.41	BG
77.	LMC B0526–6851	LI-LMC 1076	0.797	160.2	-0.19 ± 0.08	-1.85 ± 0.29	H II
78.	LMC B0526–7137	LI-LMC 1058	0.049	9.9	-0.36 ± 0.18	-2.24 ± 0.31	hii
79.	LMC B0527–6920	LI-LMC 1065	0.124	12.4	0.17 ± 0.11	-2.24 ± 0.19	H II
80.	LMC B0528–6730	LI-LMC 1090	0.563	41.4	-0.02 ± 0.07	-2.15 ± 0.17	H II
81.	LMC B0528–6905	LI-LMC 1118 (1139)	0.299	10.3	-0.51 ± 0.02	-3.75 ± 0.08	?
82.	LMC B0528–7038	LI-LMC 1101 (1098)	0.244	1.7	0.00 ± 0.02	-1.56 ± 0.59	SNR?
83.	LMC B0528–7126	LI-LMC 1106	0.063	9.1	-1.82 ± 0.19	-2.53 ± 0.27	hii
84.	LMC B0530–6651	LI-LMC 1177	0.111*	0.18	-0.39 ± 0.11	0.23 ± 0.19	?
85.	LMC B0530–6655	LI-LMC 1186	0.100	0.22	-0.82 ± 0.01	0.00 ± 0.19	SNR?
86.	LMC B0531–7106	LI-LMC 1251 (1246)	1.132	105.6	-0.13 ± 0.03	-2.26 ± 0.07	H II
87.	LMC B0532–6629	LI-LMC 1273	0.410	83.6	-0.12 ± 0.05	-2.38 ± 0.10	H II
88.	LMC B0532–6734	LI-LMC 1288	0.093	6.6	-0.56 ± 0.02	-2.57 ± 0.32	SNR?
89.	LMC B0532–6743	LI-LMC 1274 (1292)	0.770	113.8	-0.32 ± 0.09	-2.47 ± 0.10	H II
90.	LMC B0532–6826	LI-LMC 1293 (1284)	0.012*	31.9		-2.05 ± 0.09	hii
91.	LMC B0532–6833	LI-LMC 1249	0.676	20.7	0.06 ± 0.17	-2.04 ± 0.30	H II
92.	LMC B0533–6921	LI-LMC 1314	0.012*	10.3		-2.47 ± 0.40	hii
93.	LMC B0533–6948	LI-LMC 1298	0.120*	70.4	-0.39 ± 0.25	-2.06 ± 0.20	hii
94.	LMC B0534–6615	LI-LMC 1337	0.175	6.7	-0.49 ± 0.04	-2.18 ± 0.11	hii
95.	LMC B0534–6726	LI-LMC 1331	0.443	4.1	-1.66 ± 0.26	-2.07 ± 0.18	hii
96.	LMC B0534–6847	LI-LMC 1323	0.163	64.2	-1.73 ± 0.20	-2.13 ± 0.13	H II
97.	LMC B0534–6911	LI-LMC 1342	0.705*	0.5	0.10 ± 0.24	-0.55 ± 0.19	hii
98.	LMC B0535–6603	LI-LMC 1376	0.701	43.3	-0.59 ± 0.05	-2.08 ± 0.06	SNR
99.	LMC B0535–6736	LI-LMC 1367	1.454	265.0	-0.34 ± 0.08	-2.13 ± 0.18	H II
100.	LMC B0535–6948	LI-LMC 1358	0.332	4.1	0.13 ± 0.05	-1.84 ± 0.26	H II
101.	LMC B0536–6735	LI-LMC 1392		33.1	-0.38 ± 0.02	-2.67 ± 0.12	SNR
102.	LMC B0536–6914	LI-LMC 1383 (1388)	4.536	124.2	-0.06 ± 0.09	-2.55 ± 0.21	SNR
103.	LMC B0536–6934	LI-LMC 1403	0.162	29.0	0.01 ± 0.07	-2.30 ± 0.23	hii
104.	LMC B0536–6941	LI-LMC 1397	0.491	78.7	-0.40 ± 0.28	-2.11 ± 0.05	H II
105.	LMC B0537–6506	LI-LMC 1887	0.035	0.4		-0.79 ± 0.28	BG?
106.	LMC B0537–6623	LI-LMC 1422 (1426)	0.328	28.2	-0.10 ± 0.07	-2.56 ± 0.14	H II
107.	LMC B0537–6914	LI-LMC 1429	1.510*	41.4	-0.02 ± 0.05	-2.27 ± 0.13	?
108.	LMC B0538–6911	LI-LMC 1448	3.571	124.2	-0.14 ± 0.06	-2.18 ± 0.10	SNR
109.	LMC B0538–6956	LI-LMC 1460	0.213	4.1	-0.67 ± 0.52	-1.92 ± 0.34	?
110.	LMC B0538–7042	LI-LMC 1471	0.140	41.4	-0.07 ± 0.09	-1.99 ± 0.10	hii
111.	LMC B0539–6907	LI-LMC 1469	35.79	2794.5	-0.12 ± 0.04	-1.83 ± 0.21	H II
112.	LMC B0539–6931	LI-LMC 1490 (1483)	1.272	248.4	-0.01 ± 0.09	-2.09 ± 0.20	H II
113.	LMC B0540–6927	LI-LMC 1507	0.012*	41.4		-2.52 ± 0.21	hii
114.	LMC B0540–6940	LI-LMC 1503	1.939	662.4	-0.07 ± 0.04	-1.91 ± 0.22	H II
115.	LMC B0540–6946	LI-LMC 1518 (1501)	4.186	414.0	-0.17 ± 0.01	-2.47 ± 0.20	H II
116.	LMC B0540–7111	LI-LMC 1521 (1505)	0.081	61.7	-0.06 ± 0.06	-2.05 ± 0.05	hii
117.	LMC B0541–7003	LI-LMC 1544	0.045	5.4	0.11 ± 0.24	-2.33 ± 0.27	H II
118.	LMC B0541–7025	LI-LMC 1562	0.440	6.2	-0.82 ± 0.14	-2.05 ± 0.22	hii
119.	LMC B0541–7034	LI-LMC 1551	0.212	6.2	-0.12 ± 0.08	-2.22 ± 0.16	hii
120.	LMC B0542–6702	LI-LMC 1568	0.126	2.9	0.30 ± 0.18	-2.14 ± 0.34	SNR?
121.	LMC B0542–6906	LI-LMC 1594	0.798	20.7	0.33 ± 0.11	-1.74 ± 0.21	H II
122.	LMC B0542–7121	LI-LMC 1577	0.263	53.0	-0.13 ± 0.15	-2.28 ± 0.08	H II
123.	LMC B0543–6752	LI-LMC 1605	0.253	12.0	-0.03 ± 0.06	-2.08 ± 0.12	H II
124.	LMC B0543–6946	LI-LMC 1609	0.238	58.0	-0.15 ± 0.07	-2.29 ± 0.17	H II
125.	LMC B0544–6720	LI-LMC 1650	0.099	14.5	-0.39 ± 0.01	-2.12 ± 0.22	H II
126.	LMC B0545–6947	LI-LMC 1675	0.079	33.1	0.33 ± 0.24	-2.02 ± 0.26	hii
127.	LMC B0546–6934	LI-LMC 1696	0.160	11.2	-0.02 ± 0.01	-2.19 ± 0.17	hii
128.	LMC B0549–7004	LI-LMC 1744	0.699	58.4	0.09 ± 0.07	-2.57 ± 0.06	H II
129.	LMC B0556–6814	LI-LMC 1791	0.099	9.9	-0.74 ± 0.06	-2.37 ± 0.24	hii?snr
130.	LMC B0603–7102	LI-LMC 1819	0.042	5.0	-0.56 ± 0.17	-1.43 ± 0.40	bg

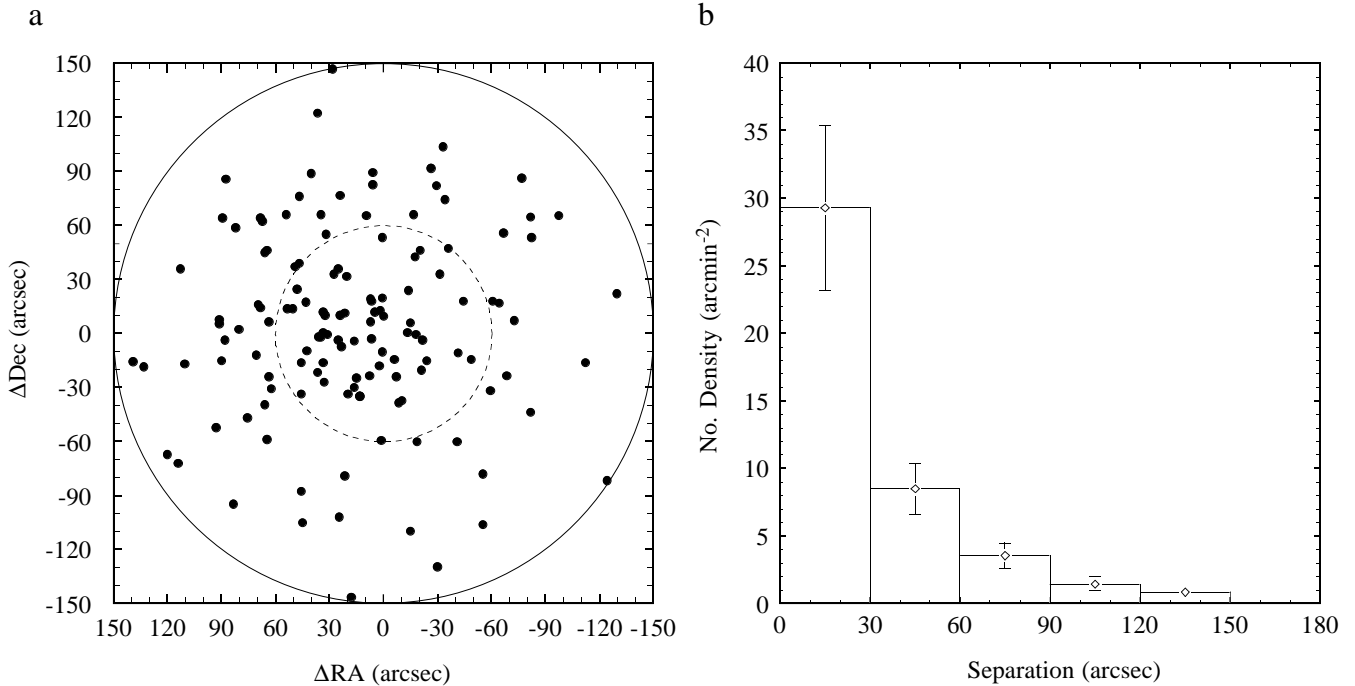


Fig. 1. a) The differences between radio and IR source positions for the LMC. The mean offset (radio-IR) is $16'' \pm 5''$ and $4'' \pm 5''$ in RA and Dec, respectively. The standard deviations are $54''$ and $53''$, respectively. The outer circle (selection criterion) is $2.5'$ radius and the inner dashed circle is $1'$ radius. b) The number of sources as a function of radio-IR source separation towards the LMC per unit area of the radial bin (per arcmin 2)

Data for all 38 sources in common are presented in Table 2. Entries of this table follow the format of Table 1 except for Col. 4 where the 4.85-GHz flux is listed rather than the 4.75-GHz flux. Radio spectral indices are not given for eight sources which were detected at only one radio frequency and for two sources for which radio data are only available at two close frequencies (4.75 and 4.85 GHz). These sources are flagged in Col. 4. No IR spectral index is given for four SMC sources, because of their detection at only one IR frequency.

4.2. Positional differences between the SMC radio and infrared sources

Positions for all 38 SMC sources common to the radio and IR surveys have been compared in the same way as for the LMC. The results of this comparison are shown in Fig. 2. The mean differences are $-7'' \pm 9''$ (radio-IR) in RA with $SD=55''$ and $-9'' \pm 11''$ in Dec with $SD=68''$. This uncertainty is also consistent with the combined positional uncertainties for the radio (defined in Paper V) and the IR sources, and justifies the initial identification criterion of $2.5'$ (equivalent to 2.7σ in RA and 2.2σ in Dec). The distribution of radio-IR separations towards the SMC shows a significant excess for small separations like that seen for the LMC comparison (Fig. 1b), but with a smaller number of sources.

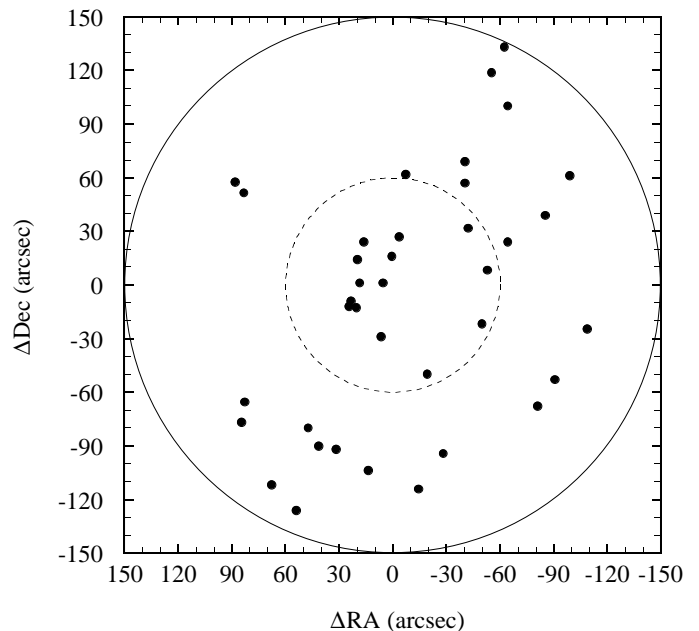


Fig. 2. The differences between radio and IR source positions for the SMC. The mean offset (radio-IR) is $-7'' \pm 9''$ and $-9'' \pm 11''$ in RA and Dec, respectively. The standard deviations are $55''$ and $68''$, respectively. The outer circle (selection criterion) is $2.5'$ radius and the inner dashed circle is $1'$ radius

Table 2. Catalogue of the SMC radio sources identified in the IRAS survey. The IR source number (Col. 3) is taken from Schwering & Israel (1990)

(1) No.	(2) Radio Source Name	(3) IR Source Name	(4) $S_{4.75}$ (Jy)	(5) $S_{60\mu\text{m}}$ (Jy)	(6) $\alpha_{\text{RAD}} \pm \Delta\alpha_{\text{RAD}}$	(7) $\alpha_{\text{IR}} \pm \Delta\alpha_{\text{IR}}$	(8) Type
1.	SMC B0018–7338	LI-SMC 226	0.107	0.6	-0.46 ± 0.06		bg
2.	SMC B0027–7409	LI-SMC 236	0.032	0.6	-0.73 ± 0.23	-2.45 ± 0.28	BG
3.	SMC B0033–7309	LI-SMC 4	0.044		0.08 ± 0.01		BG
4.	SMC B0039–7353	LI-SMC 10	0.102	0.4	0.11 ± 0.14	-3.25 ± 0.28	BG
5.	SMC B0043–7321	LI-SMC 30	0.090	14.0	0.03 ± 0.11	-2.40 ± 0.16	H II
6.	SMC B0043–7330	LI-SMC 28	0.039	17.0		-2.63 ± 0.37	snr?
7.	SMC B0044–7339	LI-SMC 35 (32)	0.057	19.0	0.61 ± 0.54	-2.15 ± 0.15	hii
8.	SMC B0045–7255	LI-SMC 40	0.020				BG?
9.	SMC B0045–7347	LI-SMC 38	0.112*	13.0	-0.18 ± 0.24	-2.01 ± 0.12	hii
10.	SMC B0046–7333	LI-SMC 45 (42)	0.264	56.0	0.11 ± 0.13	-2.24 ± 0.14	SNR
11.	SMC B0047–7332	LI-SMC 54			0.25 ± 0.06		SNR
12.	SMC B0047–7343	LI-SMC 57 (56)	0.046	14.0	0.70 ± 0.04	-2.43 ± 0.13	BG
13.	SMC B0048–7245	LI-SMC 71		2.2		-1.78 ± 0.08	hii
14.	SMC B0048–7252	LI-SMC 62	0.061	12.0	-0.61 ± 0.07	-2.31 ± 0.32	hii
15.	SMC B0048–7308	LI-SMC 65 (63)	0.523	19.0	-0.34 ± 0.04	-2.38 ± 0.42	SNR?
16.	SMC B0049–7304	LI-SMC 66		4.1	-0.12 ± 0.19	-1.89 ± 0.15	H II
17.	SMC B0049–7338	LI-SMC 68	0.046	2.8	-0.06 ± 0.36	-2.52 ± 0.38	SNR
18.	SMC B0050–7329	LI-SMC 88	0.095	9.7	-0.22 ± 0.14	-2.43 ± 0.12	H II
19.	SMC B0054–7235	LI-SMC 110 (109)	0.035	18.0	0.49 ± 0.12	-1.82 ± 0.35	snr?
20.	SMC B0056–7254	LI-SMC 124	0.121*	9.1		-2.23 ± 0.13	hii
21.	SMC B0057–7226	LI-SMC 131	1.633	200.0	-0.15 ± 0.06	-1.77 ± 0.22	SNR
22.	SMC B0100–7240	LI-SMC 153	0.083*	7.2		-2.17 ± 0.30	?
23.	SMC B0101–7210	LI-SMC 152	0.063	11.0	0.46 ± 0.23	-2.12 ± 0.14	hii
24.	SMC B0101–7221	LI-SMC 156			-3.38 ± 0.26	-0.81 ± 0.19	hii
25.	SMC B0101–7226	LI-SMC 160	0.125	4.5	-0.09 ± 0.02	-1.29 ± 0.63	SNR
26.	SMC B0102–7218	LI-SMC 162 (161)	0.411	27.0	-0.33 ± 0.19	-3.09 ± 0.07	SNR
27.	SMC B0103–7216	LI-SMC 168	0.170	45.0	0.00 ± 0.02	-1.78 ± 0.22	H II
28.	SMC B0103–7239	LI-SMC 169	0.052	1.7	-0.47 ± 0.29	-1.77 ± 0.28	SNR
29.	SMC B0104–7226	LI-SMC 170		2.1		-1.73 ± 0.39	hii
30.	SMC B0106–7215	LI-SMC 184	0.089	17.0	0.06 ± 0.22	-2.34 ± 0.21	H II
31.	SMC B0107–7327	LI-SMC 187	0.064	18.0	-0.05 ± 0.10	-2.00 ± 0.15	H II
32.	SMC B0109–7238	LI-SMC 194	0.037	4.7	-0.18 ± 0.04	-1.64 ± 0.10	H II
33.	SMC B0109–7258	LI-SMC 190	0.129	3.3	-0.63 ± 0.21	-1.50 ± 0.28	SNR?
34.	SMC B0112–7333	LI-SMC 199 (200)	0.532	46.0	0.15 ± 0.19	-2.68 ± 0.16	H II
35.	SMC B0113–7334	LI-SMC 202 (201)		32.0	0.28 ± 0.06	-2.70 ± 0.09	H II
36.	SMC B0122–7324	LI-SMC 215	0.123	55.0	0.62 ± 0.34	-1.42 ± 0.35	H II
37.	SMC B0124–7339	LI-SMC 218	0.047	2.5	0.76 ± 0.15	-1.81 ± 0.28	H II
38.	SMC B0128–7348	LI-SMC 242	0.170	11.1	-0.27 ± 0.10	-2.38 ± 0.14	H II

5. Classification and analysis of discrete sources in common to the radio and IR surveys

Out of the 130 sources common to the radio and IR surveys of the LMC (Sect. 3), 76 (58%) have been previously classified (see Table 1, Col. 8). Most are H II regions (49) and SNRs (21, including nine SNR candidates). Only six sources towards the LMC from the radio surveys are listed as background objects.

Similarly, from 38 sources common to the radio and IR surveys of the SMC (Sect. 4), 26 (68%) have been classified in previous investigations (see Table 2, Col. 8). Again, most of these sources are intrinsic to the SMC (12 H II regions and nine SNRs embedded in H II regions). Five radio/IR sources towards the SMC are listed as background.

5.1. Source classifications

Most of the MCs H II regions (and SNRs embedded in H II regions) have been detected in IR surveys. Some 95% of

H II regions in the LMC (49 out of 52) and 86% in the SMC (12 out of 14) appear as IR sources. This is not surprising as IR emission is caused by emission from the dusty surroundings of the MC sources. In Filipović et al. (1998b), we found very tight correlation between radio and H α source catalogues. Also, the similarity of broad-scale structure between radio, IR and H α emission from the MCs has been reported by Xu et al. (1992).

The comparison between radio and IR source spectral index (colour-colour diagram) did not show any correlation for different types of sources towards the MCs. Therefore this criterion is not useful in classifying sources.

From the relative number of radio sources seen in the IR frequencies that are background, compared to those that are intrinsic to the MCs, the conclusion is that the rest of the unclassified sources (54 in the LMC and 12 in the SMC) are more likely to be also intrinsic i.e. H II regions. As additional criteria, we cross-checked these sources with existing H α catalogues (Filipović et al.

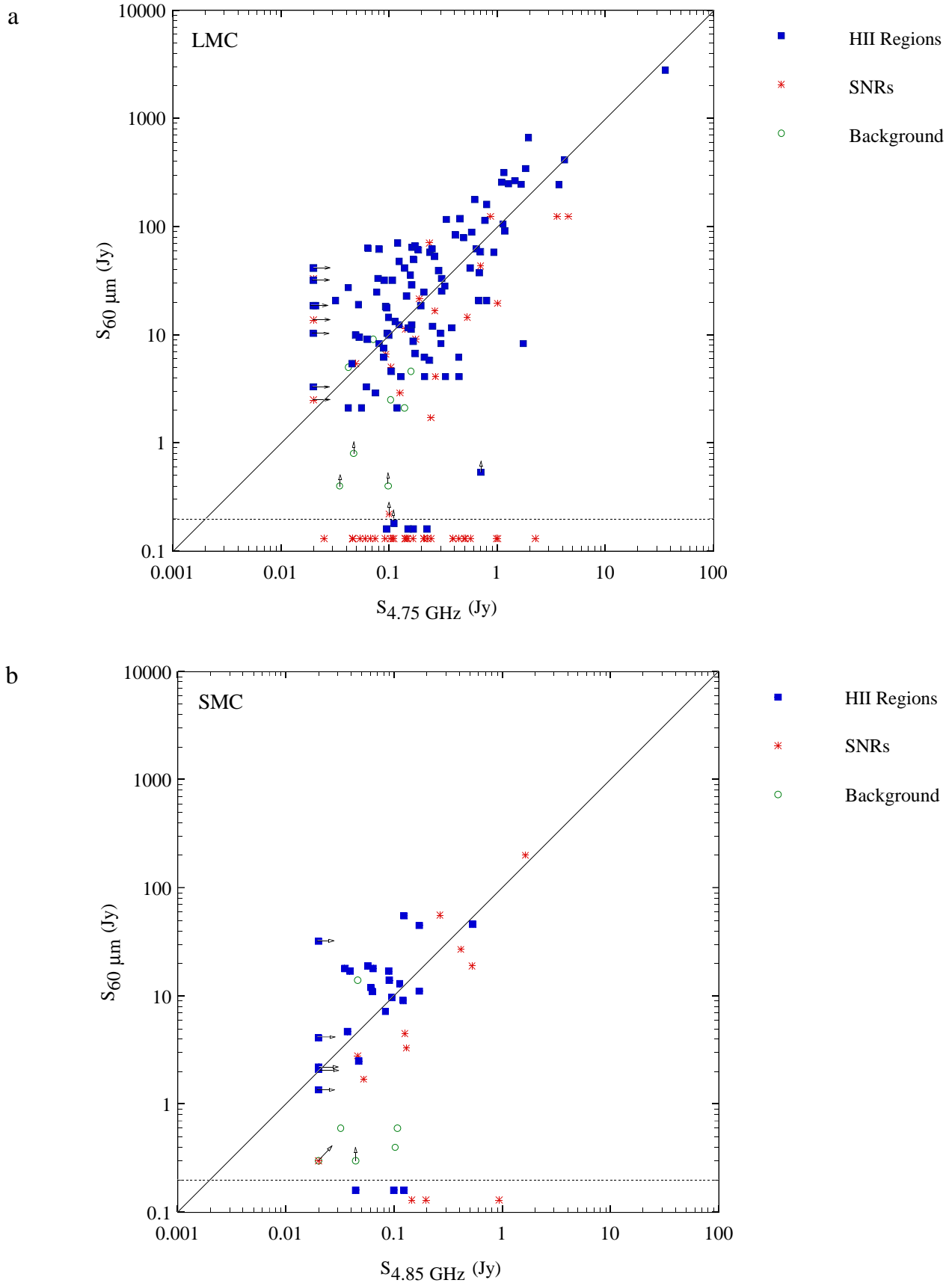


Fig. 3. The comparison of IR (60 μm) and radio flux density at 4.75 GHz (4.85 GHz for the SMC) for different classes of sources towards a) the LMC and b) the SMC. Asterisks represent SNRs; filled squares – HII Regions; and open circles – background sources. The dotted line represent the approximate threshold in radio survey. Sources below the dotted lines represents non-detections. The diagonal lines represent a ratio of $S_{60 \mu\text{m}}/S_{4.75 \text{ GHz}}=100$

1998b). However, some of these unclassified sources could be background objects.

Applying this criteria to the LMC, 40 out of 54 previously unclassified (radio to IR) sources are suggested to be intrinsic (marked in Table 1, Col. 8 as “hii”). These sources are also detected in H α surveys such as Henize (1956), DEM (Davies et al. 1976) and Kennicutt & Hodge (1986). Two sources (LMC B0433–7139 and LMC B0603–7102) are more likely to be background objects because they are well away from the LMC field defined in Paper VI and cannot be seen at any H α surveys. The other 12 sources common to radio and IR surveys remain ambiguous.

Similarly, from 12 unclassified radio and IR sources in the SMC, 10 are suggested to be H II region candidates (or SNR candidates), one is probably a background source (SMC B0018–7338) and source SMC B0100–7240 remains ambiguous (marked in Table 2, Col. 8 as “?”).

6. Radio-to-infrared source flux density comparison

The IR and the radio continuum images of the MCs are found to be closely correlated, in the sense of an overall coincidence of peaks of emission and a strong resemblance around giant star-formation regions such as 30 Doradus (Xu et al. 1992). Similar correlations are found in other disk galaxies (Wunderlich & Klein 1988 and references therein). Here, we will concentrate on the comparison between discrete source flux densities from these two wavelengths.

The comparison between the source radio flux density at the 4.75-GHz survey (4.85-GHz survey for the SMC) and the IR survey at 60 μ m is shown in Figs. 3a and 3b for the LMC and SMC respectively. Here, three groupings of sources are clearly identified. A group of H II regions, SNRs and background sources which are strong at both frequencies and with a good correlation of flux densities with a spread of $\sim 20\%$ (after allowing for the radio flux density to be $\sim 1\%$ of the IR due to the mean spectra between these frequencies). From the 53 previously studied H II regions in the LMC, 49 IR sources were found to be associated with these sources. Also, from the 26 known SMC H II regions, 23 IR sources have counterparts in radio surveys. A similar situation can be found for SNRs embedded in H II regions.

Two other groups representing strong sources at IR or radio frequencies, but which are not detected at radio and IR frequencies, are also present. These sources fall below the sensitivity limits of the catalogues.

Most of the sources that fall below the IR cut-off are “uncontaminated” radio SNRs that are known to be low in IR emission. This type of graphical representation serves well to identify these objects. The ratio of IR-quiet to IR-loud SNRs is 21 to 37 ($\sim 36\%$) for the LMC and 11 to 9 ($\sim 55\%$) for the SMC. A small number of H II regions were also not found, probably because of confusion within the IR surveys.

Several radio-loud objects are plotted as lower limits, as exact flux densities at 4.75 GHz (4.85 GHz for the SMC) are not known (Sect 3.1). In addition, there are many IR detections (~ 1000 for the LMC) for which there is no confidently ascribed radio counterpart. We treat these objects less seriously as many of these detections may be spurious (as noted above) and they are not plotted in Figs. 3a and 3b.

7. Conclusions

The comparison of Parkes radio surveys with the IRAS IR surveys showed 130 and 38 sources in common to the LMC and SMC respectively. Most of these sources ($\sim 90\%$) are intrinsic to the MCs as H II regions and SNRs. Some 40 new sources in the LMC and 10 sources in the SMC are classified on this basis as H II region candidates. A flux density comparison of the sources in common for the radio and IR surveys shows very good correlation for the sources intrinsic to the MCs.

Acknowledgements. We thank M. Hunt, D. Goddard, J. Lequeux and L. Staveley-Smith for considerable help and comments in manuscript.

References

- Davies R.D., Elliott K.H., Meaburn J., 1976, Mem. R. astr. Soc. 81, 89
- Filipović M.D., Haynes R.F., White G.L., et al., 1995, A&AS 111, 311 (Paper IV)
- Filipović M.D., 1996, PhD Thesis, University of Western Sydney, Nepean
- Filipović M.D., White G.L., Haynes R.F., et al., 1996, A&AS 120, 77 (Paper IVa)
- Filipović M.D., Haynes R.F., White G.L., et al., 1997, A&AS 121, 321 (Paper V)
- Filipović M.D., Haynes R.F., White G.L., Jones P.A., 1998a, A&AS (in press) (Paper VII)
- Filipović M.D., Jones P.A., White G.L., Haynes R.F., 1998b, Proc. ASA (in press)
- Henize K.G., 1956, ApJS 2, 315
- Kennicutt R.C., Hodge P.W., 1986, ApJ 306, 130
- Meylnik M., Rice W., 1990, High Resolution (HiRes) Processing, in IPAC Users Guide
- Schwering P.B.W., 1989, A&AS 79, 79
- Schwering P.B.W., Israel P.F., 1989, A&AS 79, 105
- Schwering P.B.W., Israel P.F., 1990, Atlas and Catalogue of Infrared Sources in the Magellanic Clouds. Kluwer, Dordrecht
- Wunderlich E., Klein U., 1988, A&A 206, 47
- Xu C., Klein U., Meinert D., Wielebinski R., Haynes R.F., 1992, A&A 257, 47